MRS Communications (2018), *8*, 878–884
© Materials Research Society, 2018
doi:10.1557/mrc.2018.86

MRS Communications

Research Letter

Improving ambient stability of BiI_3-based perovskites using different phosphoniums as the organic cation

Diana F. Garcia-Gutierrez, Universidad Autónoma de Nuevo León, UANL, Fac. de Ciencias Químicas, FCQ, Av. Universidad S/N, Cd. Universitaria, San Nicolás de los Garza, Nuevo León, C.P. 66450, México; Universidad Autónoma de Nuevo León, UANL, Fac. de Ingeniería Mecánica y Eléctrica, FIME, Av. Universidad S/N, Cd. Universitaria, San Nicolás de los Garza, Nuevo León, C.P. 66450, México; Universidad Autónoma de Nuevo León, UANL, División de Estudios de Posgrado FCQ, Guerrero y Progreso S/N, Col. Treviño, Monterrey, Nuevo León, C.P. 64570, México
Domingo I. Garcia-Gutierrez, Universidad Autónoma de Nuevo León, UANL, Fac. de Ingeniería Mecánica y Eléctrica, FIME, Av. Universidad S/N, Cd. Universitaria, San Nicolás de los Garza, Nuevo León, C.P. 66450, México
Diego González-Quijano, Universidad Autónoma de Nuevo León, UANL, Fac. de Ciencias Químicas, FCQ, Av. Universidad S/N, Cd. Universitaria, San Nicolás de los Garza, Nuevo León, C.P. 66450, México; Universidad Autónoma de Nuevo León, UANL, División de Estudios de Posgrado FCQ, Guerrero y Progreso S/N, Col. Treviño, Monterrey, Nuevo León, C.P. 64570, México
Itzel A. Abarca-Villarreal and **Sofia F. Galindo-Garza,** Universidad Autónoma de Nuevo León, UANL, Fac. de Ciencias Químicas, FCQ, Av. Universidad S/N, Cd. Universitaria, San Nicolás de los Garza, Nuevo León, C.P. 66450, México
Eduardo M. Sanchez, Universidad Autónoma de Nuevo León, UANL, Fac. de Ciencias Químicas, FCQ, Av. Universidad S/N, Cd. Universitaria, San Nicolás de los Garza, Nuevo León, C.P. 66450, México; Universidad Autónoma de Nuevo León, UANL, División de Estudios de Posgrado FCQ, Guerrero y Progreso S/N, Col. Treviño, Monterrey, Nuevo León, C.P. 64570, México

Address all correspondence to Eduardo M. Sanchez at **eduardo.sanchezcv@uanl.edu.mx**

(Received 9 February 2018; accepted 17 April 2018)

Abstract

Perovskites solar cells have reached impressive efficiencies (22%) in recent years. Because certain environmental concerns are raised by the use of lead halides, there is an interest to seek out lead-free alternatives, featuring bismuth or antimony. Alongside, one of the major drawbacks displayed by $MAPbI_3$ is their low stability at ambient conditions. In this work, $(RP_4)_xBi_yI_z$ were synthesized, using different types of tetra-alkylphosphoniums (R_4PI) were R = ethyl, butyl, hexyl, and octyl, to assess their stability. Afterwards, they were characterized to study their morphology and crystal structure, as well as their optical properties.

Introduction

Perovskite solar cells are now positioned among the most researched topics in recent years, due to the increment in their power conversion efficiency, which has improved from 10% to over 22% in the last 7 years.[1] Among the materials most frequently reported for this application, the lead halides (PbI_2, PbCl) combined with methyl ammonium iodide (MAI) can be found.[2–4] The perovskites structures formed combining this organic cation and the lead halides display high charge carriers' mobilities, long diffusion lengths, high absorption optical coefficients, and ease of processing at low temperatures (≤100 °C).[3–5] Unfortunately, environmental requirements demanding the replacement of Pb in a wide variety of applications are forcing this recent research topic to look for alternative inorganic halides to synthesize these promising hybrid perovskites structures. On the other hand, these hybrid materials also show poor ambient stability, mainly related to humidity, which causes the degradation of the structure and the loss of the properties previously described; producing photovoltaic (PV) devices that last only a few minutes at ambient and working conditions. Different strategies have been implemented trying to improve the ambient stability of these perovskite materials; among these strategies, the replacement of the hole transport layer, device encapsulation, partial or full replacement of the MAI organic cation, to the most recent approach of combining bi-dimensional with three-dimensional perovskites structures can be mentioned.[6–8]

Given the wide variety of organic-BiI_x compounds reported by Mitzi; Mitzi and Brock[9,10] and the fact that BiI_3 has been proved as a non-toxic material, stable at ambient conditions and with acceptable optoelectronic properties for PV applications,[11] it has been proposed to replace PbI_2 as the inorganic part of the perovskite structure, in order to reduce the possible environmental impact these devices might have in the future. On the other hand, in this work it is proposed to replace the MAI for different tetra-alkylphosphoniums as the alternative organic cation, as a possible solution to solve the ambient stability problem displayed by the perovskites based on $MAPbI_2$.

The proposed phosphonium salts belong to a family of compounds referred to as ionic liquids (ILs). Among the general properties displayed by these ILs, the following can be highlighted: their low vapor pressure, high thermal stability, ability to dissolve a wide variety of organic and inorganic compounds,

https://doi.org/10.1557/mrc.2018.86 Published online by Cambridge University Press

high hydrophobicity,[12] ease of functionalization, wide range of liquid state, high effective concentrations, ability to flow, wide electrochemical windows, and high ionic conductivity.[13,14] It has been reported that the number of possible combinations of potential anion–cation for these ILs is around one trillion (10^{12}).[15] Among the reported ILs in the literature, we can find the cation base-*N*, as the *N*-methylimidazolium and the pyrrolidinium salts, as well as the ammoniums, pyridiniums, pycoliniums, and the phosphonium salts.[12,14–17] The phosphonium ILs can be used as solvents, electrolytes, thermal fluids, phase transfer catalysts, and very recently are being studied for potential applications in PV devices.[12–18] There are few reports on the use of phosphonium iodides in the perovskites solar cells; however, Mostafa *et al.*[19,20] reported the synthesis of perovskites structures using methyl triphenylphosphonium and Mn, Cu, and Hg halides.

In the current work, the synthesis and physical characterization of four new hybrid compounds, of the organic–inorganic type, were performed. As the organic phase, four tetraalkylphosphonium iodide salts (R_4PI, R = ethyl, butyl, hexyl, and octyl) were used, in order to asses which of the different phosphonium salts provided the new hybrid material with the highest ambient stability, based on their different hydrophobicity; whereas bismuth (III) iodide was used as the inorganic phase (BiI_3). The synthesized hybrid compounds were characterized by means of x-ray diffraction (XRD), UV–vis absorption, photoluminescence (PL), Fourier transformed infrared spectroscopy (FTIR) and scanning electron microscopy (SEM). The stability at ambient conditions of the hybrid materials was monitored using XRD after exposure to ambient conditions up to 4 months in some systems.

Materials and methods

Organic–inorganic perovskites synthesis

Materials

Bismuth iodide (III) (BiI_3, Aldrich 99%), tetraethylphosphonium iodide (E_4PI, as-synthesized), tetrabutylphosphonium iodide (B_4PI, as-synthesized), tetrahexylphosphonium iodide (H_4PI, as-synthesized), tetraoctylphosphonium iodide (O_4PI, as-synthesized), *N*,*N*-dimethylformamide (DMF, Aldrich).

Procedure

Organic–inorganic perovskites $(RP_4)_xBi_yI_z$ synthesis was carried out in a globe box filled with N_2. In a direct reaction, 0.59 mmol of BiI_3 was mixed with 0.59 mmol of the organic cation R_4PI in 2 mL of DMF maintaining a molar relationship of 1 : 1. Heat and stir conditions were 110 °C and 7 h for $(EP_4)_xBi_yI_z$ composite; same temperature and 24 h for $(BP_4)_xBi_yI_z$ and $(OP_4)_xBi_yI_z$; and 60 °C was used for the $(HP_4)_xBi_yI_z$ composite and 72 h of stirring.

Thin films fabrication

Hybrid composites in the solution were filtrated with a 0.45 μL PTFF filter; then, 200 μL of the filtered solution was spin coated on a 2.4 × 2.4 cm^2 cleaned glass substrate at 2000 rpm for 55 s. Finally, the thin films deposited were thermally treated (TT) at different temperatures, one sample of each system was crystalized at an ambient temperature (25 °C); while the TT varied from 60 to 200 °C in some cases.

Spin coating and TT were carried out inside a globe box; the samples were taken out of the globe box for their characterization and stability test.

Stability test

XRD characterization of thin films were performed in a Bruker D2 Phaser x-ray diffractometer with Cu K_α radiation (λ = 1.5418 Å) and a position-sensitive LynxEye detector. The diffraction studies were performed from 5° to 90° in two-theta angle with a step size of 0.05°/s. The thin films of 400–600 nm in thickness deposited on top of a glass substrate of 2.4 × 2.4 cm were XRD measured immediately after taken out of the globe box, then they were stored at ambient conditions (25 °C, normal illumination, and 40% of humidity) until following analysis. The samples were tested at 1, 24, and 168 h after being synthesized; finally, they were tested every 2 weeks until the perovskite started to show signs of degradation.

Results

Figure 1(a) shows the UV–vis absorption and PL spectra of the $(RP_4)_xBi_yI_z$ compounds. The hybrid materials display maximum absorption and emission peaks at around 439 and 567 nm for R = octyl; 441 and 568 nm for R = ethyl and hexyl, respectively; 442 and 537 nm for R = butyl, showing a red shift of ~20 nm in the absorption peak compared with the BiI_3 precursor, which shows a maximum UV-Vis absorption peak at ~426 nm with a maximum emission peak at ~568 nm. Regardless this small difference, the absorption and emission spectra for the $(RP_4)_xBi_yI_z$ compounds are very similar to the BiI_3 precursor. The optical response of BiI_3 is associated with its electronic structure, which is characterized by its highest valence bands and the ensemble of the lowest conduction bands, corresponding mainly to *s*- and *p*-states of the two Bi atoms found in the unit cell of the hexagonal crystal structure.[21] The valence band is mainly composed by the *s*-states of Bi, with the admixture of some I *p*-state-like and I sp^3 hybrid type; whereas the conduction band is mainly formed from Bi *p*-states with the admixture of I *s*-states.[21] Based on the similarity between the absorption and emission spectra for the $(RP_4)_xBi_yI_z$ compounds and its Bi precursor, it is suggested that the electronic structure of the synthesized compounds would be similar to the one displayed by its precursor; with a valence band showing a strong Bi *s*-state character, admixed with I *p*-state and I sp^3 hybrid-type states; while the conduction band displays a more Bi *p*-state character, admixed with I *s*-state.

The transmittance spectra obtained for the different hybrid material systems synthesized are shown in Fig. 1(b). It is worth mentioning that the spectra displayed in the figure correspond to those samples that showed the highest stability to ambient conditions (25 °C and 40% humidity) among the

https://doi.org/10.1557/mrc.2018.86 Published online by Cambridge University Press

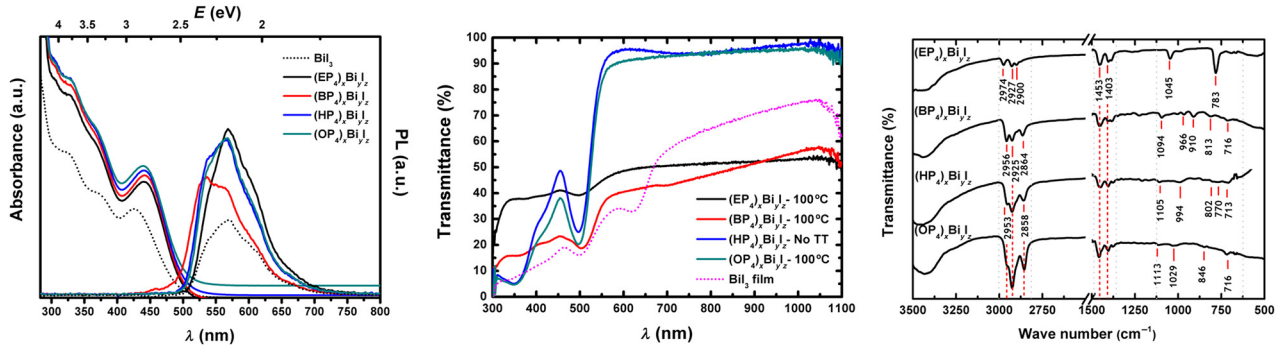


Figure 1. (a) UV–vis absorption and PL spectra of the synthesized hybrid compounds, (b) transmittance spectra corresponding to the most stable sample to ambient conditions of the different hybrid material systems synthesized, and (c) FTIR spectra of the synthesized hybrid materials.

different hybrid systems. A transmittance of ~50%, in all the analyzed range, was observed for the $(BP_4)_xBi_yI_z$ and $(EP_4)_xBi_yI_z$ samples, which decreases at ~496–506 nm. The other two hybrid systems showed a higher transmittance (~90%), down to ~500 nm, where it starts to clearly decrease. The optical energy band gap was calculated for these hybrid materials, obtaining values within the range of 1.8–2.3 eV. These differences in the optical band gap could be related to atomic arrangement variations in the structure of the synthesized hybrid materials.

The FTIR spectra acquired for the different hybrid materials synthesized are shown in Fig. 1(c). Three regions of the spectra, with bands characteristic of each system, can be observed. These regions in the spectra are indicated in the figure by gray-dotted lines. Three bands can be observed in the range between 3000 and 2850 cm^{-1}, and they can be associated with the stretching signals of the C–H alkyl groups; it is worth noting in this region the small differences in wave number value depending on the size of the alkyl chain used, also the intensities of the peaks increase as the alkyl chain increases in length. In the second region, the bands at ~1454, 1400, and a small shoulder at 1312 cm^{-1} remain constant for the four hybrid compounds; these bands are also related to C–H groups and they can be associated with the symmetric and asymmetric wobbling of CH_3 groups. Finally, in the third region observed in the range between 1125 and 625 cm^{-1}, there is a band associated with the C–P bond at 1045 cm^{-1} for R = ethyl and this band showed a shift to 1094, 1105, and 1113 cm^{-1} as the alkyl chain increases; the bands at ~716 and 713/cm^{-1} correspond to the $–CH_2–$ stretching; finally, the other bands in the range between 1000 and 650 cm^{-1} could be related to the C–H bond of alkenes compounds.[22–24]

The diffractograms of the synthesized hybrid materials are shown in Fig. 2. Thin films of the hybrid compounds were deposited by spin coating, it is worth mentioning that thermal treatments were performed at different temperatures, from 80 to 200 °C, to selected samples, and the diffractograms displayed in Fig. 2 correspond to those samples that showed the best morphologic quality along with the highest stability at ambient conditions, assessed as well by XRD measurements at different ambient exposure times. The diffractograms shown in Fig. 2 were acquired immediately after performing the indicated thermal treatment on the samples, and taking them out of the glove box. It can be observed that highly crystalline thin films were obtained, with clear signals between 5° and 60° in 2θ. In some cases, for example, the hexyl system, the most stable thin film to ambient conditions was the sample with no thermal treatment, this sample crystallized at ambient temperature. The diffractogram corresponding to the precursor showed peaks that were related to the "rhombohedral" crystal structure of BiI_3 (JCPDS 48-1795), while the rest of the diffractograms could not be associated with any existing JCPDS card. After a thorough literature revision, a reference reporting the crystal structure of a similar compound was found.[25] In that study, the organic cation used was methyl-phosphonium (PMe_3), while the inorganic anion was $BiBr_3$; the crystal structure of this hybrid compound was determined by means of single-crystal XRD studies, and the result obtained was an "orthorhombic" crystal system with the following lattice parameters:

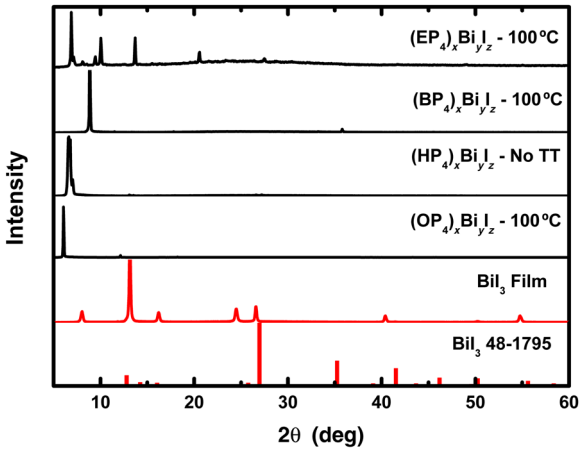


Figure 2. Diffractograms of the indicated synthesized hybrid materials and the BiI_3 precursor.

https://doi.org/10.1557/mrc.2018.86 Published online by Cambridge University Press

Table I. Lattice parameters calculated for the possible crystal structure solutions for the different hybrid materials.

Sample	a_0 (Å)	b_0 (Å)	c_0 (Å)	α	β	γ
(Ethyl-P_4)$_x$Bi$_y$I$_z$	13.20	22.37	10.58	100.31°	97.72°	101.72°
(Butyl-P_4)$_x$Bi$_y$I$_z$	10.47	10.47	25.41	90°	90°	90°
(Hexyl-P_4)$_x$Bi$_y$I$_z$ (1)	13.27	13.27	20.29	90°	90°	90°
(Hexyl-P_4)$_x$Bi$_y$I$_z$ (2)	13.53	40.13	3.46	90°	90°	90°
(Octyl-P_4)$_x$Bi$_y$I$_z$ (1)	7.44	7.44	16.18	90°	90°	90°
(Octyl-P_4)$_x$Bi$_y$I$_z$ (2)	10.95	14.96	4.35	90°	90°	90°
(Octyl-P_4)$_x$Bi$_y$I$_z$ (3)	8.09	12.75	7.45	90°	90°	90°

$a_0 = 8.03$ Å, $b_0 = 20.54$ Å, and $c_0 = 10.37$ Å. Single-crystal XRD studies are being performed to determine the crystal structure of the different synthesized hybrid materials in this study. However, in order to obtain preliminary information regarding the crystal structure of the synthesized (RP$_4$)$_x$Bi$_y$I$_z$ compounds, ab initio structure solution studies were performed using the software EXPO2014.[26] Lattice parameters obtained from these structure calculations are presented in Table I. For the case of the hybrid material with R = ethyl, this ab initio study provided a solution for a "triclinic" crystal system; for the case R = butyl, a solution was obtained for a "tetragonal" crystal system; in the case for R = hexyl, two plausible solutions were calculated, (1) for a "tetragonal" crystal system and another (2) for an "orthorhombic" crystal system; while for the case where R = octyl, three plausible solutions were calculated, (1) for a "tetragonal" crystal system, (2) another one for an "orthorhombic" crystal system, and the last one (3) also for an "orthorhombic" crystal system, with different lattice parameters than the previous solution.

These possible structures need to be confirmed by the results obtained from the single-crystal XRD studies that are being currently performed in our research group, to determine the actual crystal structure displayed by the hybrid materials synthesized.

In the SEM images of Fig. 3, the different morphologies adopted by the four different synthesized compounds when crystalizing can be observed. Images to the left correspond to secondary electrons signal, and images to the right correspond to the backscattered electrons signal (BSE). For the system with R = ethyl [Figs. 3(a) and 3(b)], the shortest alkyl chain used, crystals with irregular morphology and sizes between 15 and 30 μm were obtained. The difference in contrast observed in the BSE image could be related to the difference in the thickness of the crystals in different places. For the system with R = butyl [Figs. 3(c) and 3(d)], linear crystals with ~5 μm wide by a few hundred micrometer long were obtained, although a non-continuous film is observed; however, a homogeneous distribution and a homogeneous composition of the crystals in the film can be seen, according to the BSE information; it is worth mentioning that at lower thermal treatment temperature, the size of the crystals decreased. For the hybrid materials synthesized with R = hexyl [Figs. 3(e) and 3(f)] and octyl [Figs. 3(g) and 3(h)], a homogeneous film was observed with several surface defects. In Figs. 3(e) and 3(f), a homogeneous composition of the film can be observed; the small crystals on the surface of the thin film [inset of Fig. 3(e)] display a higher intensity [inset of Fig. 3(f)] compared with the rest of the thin film; this contrast can be attributed to the difference in thickness related to the presence of the small crystals above the thin film. In Fig. 3(h), a clear difference in composition can be observed; the dark "sheets" on the surface of the thin film can be associated with the presence of unreacted organic cation precursor. The change in morphology from the synthesized perovskite with the shortest organic cation to the longest one can be attributed to the relationship between the crystalline structure and the final crystal shape.[27] As it can be seen in Figs. 3(a) and 3(b), the shape of the crystals made of (EP$_4$)$_x$Bi$_y$I$_z$ is irregular with a star-like shape, which can be related to the possible triclinic crystal structure as predicted from our XRD simulation results. The linear crystals shown in Figs. 3(c) and 3(d) made of (BP$_4$)$_x$Bi$_y$I$_z$ can be attributed to the possible tetragonal crystal structure predicted by our XRD simulation results. Finally, the more continuous films made of (HP$_4$)$_x$Bi$_y$I$_z$ and (OP$_4$)$_x$Bi$_y$I$_z$, shown in Figs. 3(e)–3(h), respectively, can be attributed to the possible orthorhombic crystal structure, as predicted from our XRD simulation results.

XRD results for the (RP$_4$)$_x$Bi$_y$I$_z$ samples show an increment in the intensity of their diffraction peaks after exposure to ambient conditions. These observations imply an improvement of the crystallinity in the samples, which correlates to an improve stability for environmental conditions. The results obtained show how replacing the methyl ammonium organic phase by the R_4PI phase considerably increases the ambient stability of the hybrid composite. Figure 4 shows the stability results until today. For the hybrid compounds synthesized with ethyl- and butyl-phosphonium [Figs. 4(a) and 4(b), respectively] as organic cation, the thin film TT at 100 °C has shown the highest stability in the environment, displaying an increase in the intensity of its reflections and the absence of the appearance of new peaks in their diffractograms. On the other hand, for the system with hexyl-phosphonium [Fig. 4(c)], the sample

https://doi.org/10.1557/mrc.2018.86 Published online by Cambridge University Press

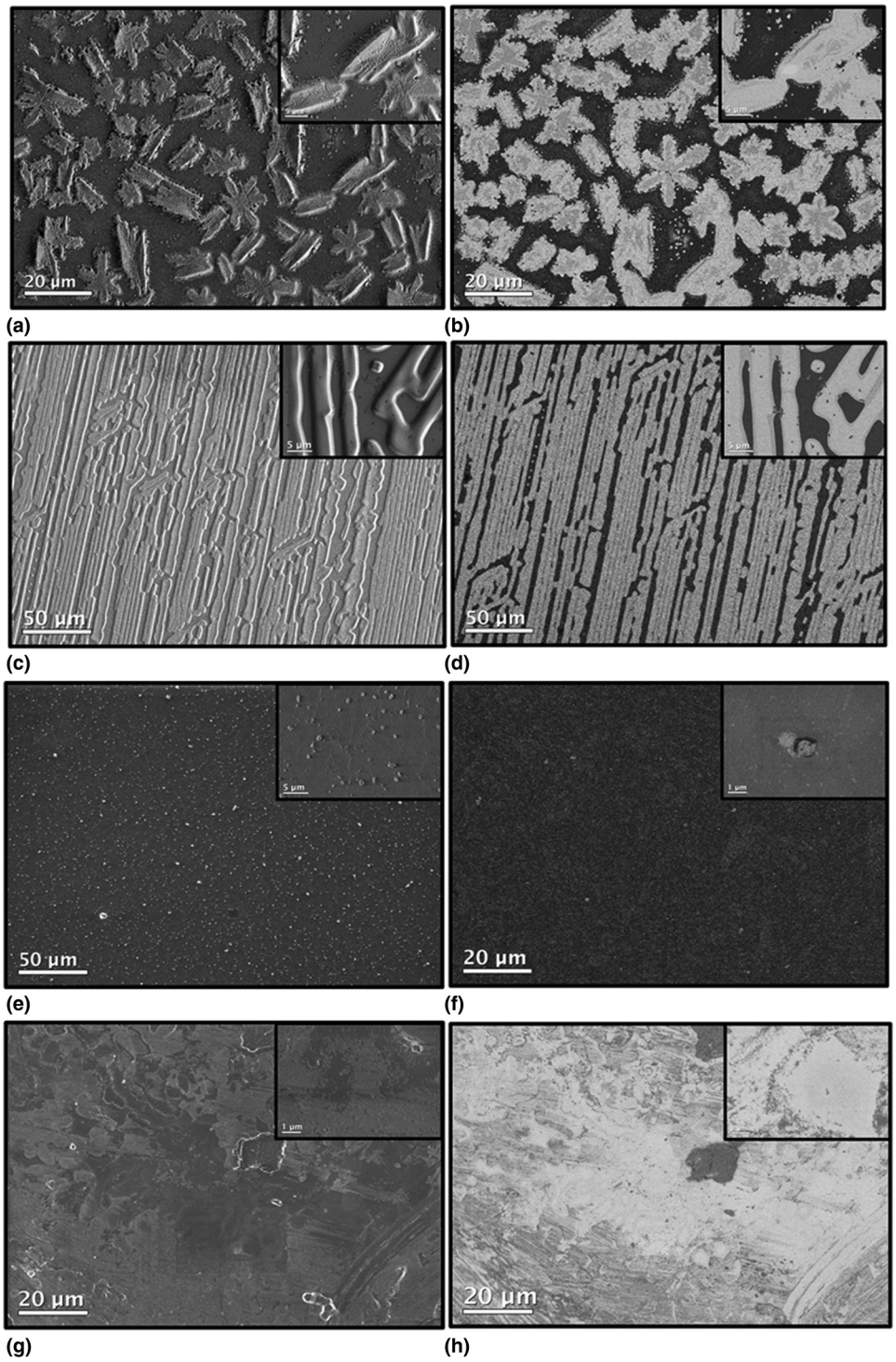


Figure 3. SEM images of the films synthesized with the hybrid compounds. (a, b) Correspond to the system with *R* = ethyl; (c, d) to *R* = butyl; (e, f) to *R* = hexyl; and finally, (g, h) to *R* = octyl.

that crystallized at room temperature is the one that has shown the highest stability for this system, since those that were TT at different temperatures have shown the formation of a new peak next to the most intense one. For the octyl-phosphonium system [Fig. 4(d)], the sample TT at 100 °C has shown the highest ambient stability for this system; however, the octyl-phosphonium sample has only been tested up to 552 h, and they have started to show a decrement in the intensity of their

https://doi.org/10.1557/mrc.2018.86 Published online by Cambridge University Press

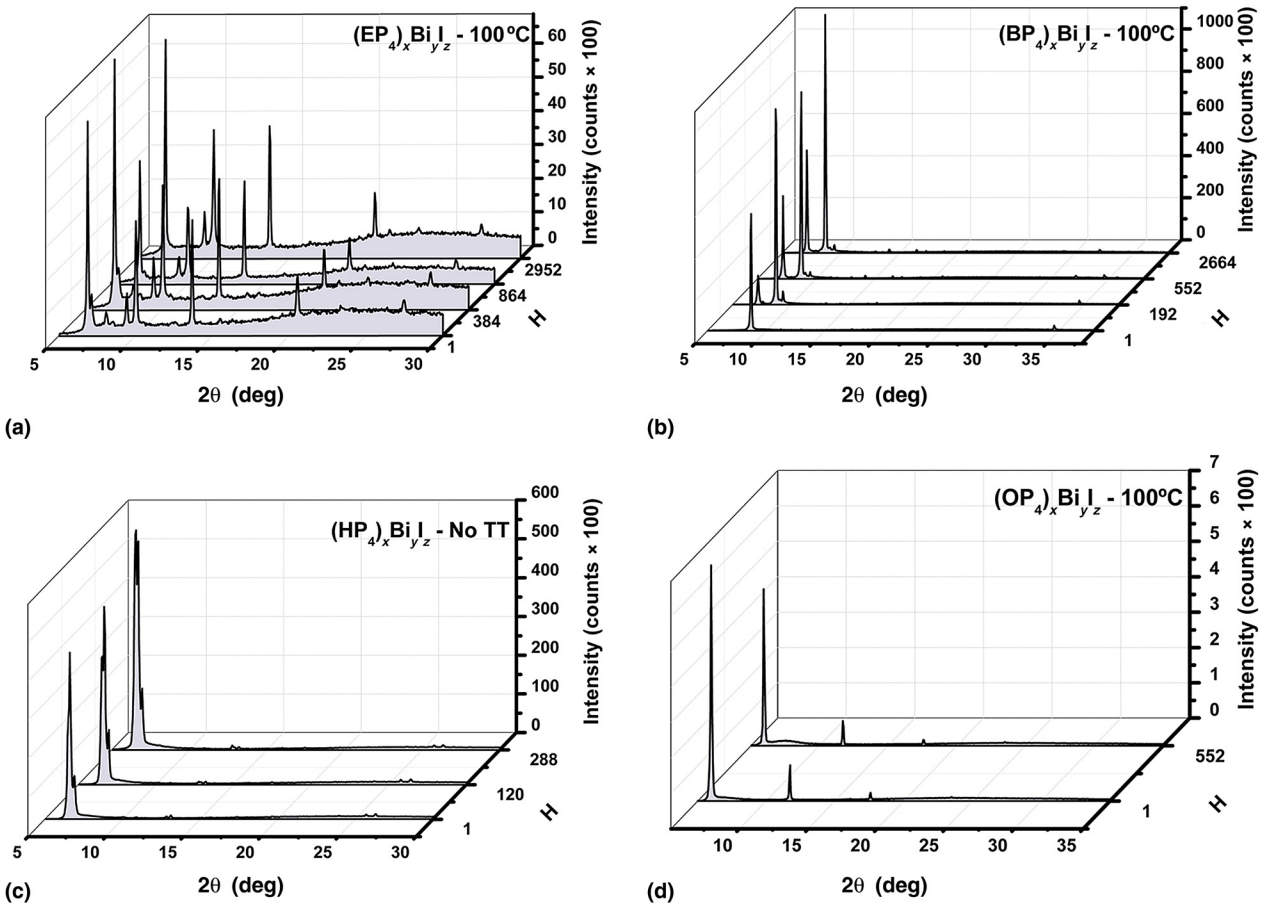


Figure 4. Diffractograms corresponding to the ambient stability test. (a) $(EP_4)_xBi_yI_z$ thermally treated at 100 °C, (b) $(BP_4)_xBi_yI_z$ thermally treated at 100 °C, (c) $(HP_4)_xBi_yI_z$ with no thermal treatment, and (d) $(OP_4)_xBi_yI_z$ thermally treated at 100 °C.

XRD peaks, which suggests that this hybrid material is less stable at ambient conditions compared with the previous three. The hybrid perovskites synthesized with the organic cations with shorter carbon chains have displayed the highest stability compared with the organic cations with longer carbon chains, which started to show a decrease in the intensity of their reflections in 2θ in less time exposed to ambient conditions.

Conclusions

BiI_3 and tetra-*n*-alkylphosphonium salts form stable and crystalline hybrid materials when synthesized by the one-step method and at low temperatures, meaning temperatures lower than 125 °C. The hybrid materials thin films were deposited by the spin coating method, which is a simple, affordable, and accessible fabrication process. The hybrid compounds show absorption and luminescence within the range of the visible spectrum, similar to the characteristics of the BiI_3 precursor. The new hybrid compounds crystallize with a long-range ordered structure, and given the results of the stability tests, the hybrid materials show increased stability to ambient conditions and humidity (25 °C, 40% humidity) up to almost 3000 h, compared with $MAPbI_3$. These hybrid materials are good candidates for absorbing layer in tandem solar cells, due to the high values of their band gap (1.8–2.3 eV). The quality of the thin films needs to be improved for future PV applications.

Acknowledgments

The authors acknowledge the financial support received through the projects 256766 CONACYT-SENER and CONACyT-FC-2015-2-1252.

References

1. Efficiency chart NREL, https://www.nrel.gov/pv/assets/images/efficiency-chart.png.
2. S. Colella, E. Mosconi, P. Fedeli, A. Listorti, F. Gazza, F. Orlandi, P. Ferro, T. Besagni, A. Rizzo, G. Calestani, G. Gigli, F. De Angelis, and R. Mosca: $MAPbI_3$—x Cl x mixed halide perovskite for hybrid solar cells : the role of chloride as dopant on the transport and structural properties. *Chem. Mater.* **25**, 4613 (2013).
3. G. Hodes: Perovskite-based solar cells. *Science* **342**, 317 (2013).
4. H.J. Snaith: Perovskites: the emergence of a new era for low-cost, high-efficiency solar cells. *J. Phys. Chem. Lett.* **4**, 3623–3630 (2013).
5. T. Song, Q. Chen, H.H.-P. Zhou, C. Jiang, H.-H. Wang, Y. (Michael) Yang, Y. Liu, J. You, Y. Yang, Y. Liu, J. You, Y. (Michael) Yang, Y. Liu, J. You,

https://doi.org/10.1557/mrc.2018.86 Published online by Cambridge University Press

and Y. Yang: Perovskite solar cells: film formation and properties. *J. Mater. Chem. A* **3**, 9032 (2015).
6. X. Zhang, X. Ren, B. Liu, R. Munir, X. Zhu, D. Yang, J. Li, Y. Liu, D. Smilgies, R. Li, Z. Yang, T. Niu, X. Wang, A. Amassian, K. Zhao, and S.F. Liu: Stable high efficiency two-dimensional perovskite solar cells via cesium doping. *Energy Environ. Sci.* **10**, 2095 (2017).
7. H. Tan, A. Jain, O. Voznyy, X. Lan, F.P. García de Arquer, J.Z. Fan, R. Quintero-Bermudez, M. Yuan, B. Zhang, Y. Zhao, F. Fan, P. Li, L. N. Quan, Y. Zhao, Z.-H. Lu, Z. Yang, S. Hoogland, and E.H. Sargent: Efficient and stable solution-processed planar perovskite solar cells via contact passivation. *Science* **355**, 722 (2017).
8. Z. Wang, Q. Lin, F.P. Chmiel, N. Sakai, L.M. Herz, and H.J. Snaith: Efficient ambient-air-stable solar cells with 2D–3D heterostructured butylammonium-caesium-formamidinium lead halide perovskites. *Nat. Energy* **6**, 17135 (2017).
9. D.B. Mitzi: Organic–inorganic perovskites containing trivalent metal halide layers: the templating influence of the organic cation layer. *Inorg. Chem.* **39**, 6107 (2000).
10. D.B. Mitzi and P. Brock: Structure and optical properties of several organic–inorganic hybrids containing corner-sharing chains of bismuth iodide octahedra. *Inorg. Chem.* **40**, 2096 (2001).
11. U.H. Hamdeh, R.D. Nelson, B.J. Ryan, U. Bhattacharjee, J.W. Petrich, and M.G. Panthani: Solution-processed BiI_3 thin films for photovoltaic applications: improved carrier collection via solvent annealing. *Chem. Mater.* **28**, 6567 (2016).
12. R.E. Ramírez and E.M. Sánchez: Molten phosphonium iodides as electrolytes in dye-sensitized nanocrystalline solar cells. *Sol. Energy Mater. Sol. Cells* **90**, 2384 (2006).
13. R.E. Del Sesto, C. Corley, A. Robertson, and J.S. Wilkes: Tetraalkylphosphonium-based ionic liquids. *J. Organomet. Chem.* **690**, 2536 (2005).
14. R.E. Ramírez, L.C. Torres-González, and E.M. Sánchez: Electrochemical aspects of asymmetric phosphonium ionic liquids. *J. Electrochem. Soc.* **154**, B229 (2007).
15. K.J. Fraser and D.R. MacFarlane: Phosphonium-based ionic liquids: an overview. *Aust. J. Chem.* **62**, 309 (2009).
16. R.E. Ramírez-Garcia and E.M. Sánchez-Cervantes: Desarrollo de nuevos electrolitos con potencial uso en celdas solares nanocristalinas. *Cien. UANL* **X**, 400 (2007).
17. R.E. Ramírez, L.C. Torres-González, A. Hernández, A. García, and E. M. Sánchez: Conductivity and viscosity behavior of asymmetric phosphonium iodides. *J. Phys. Chem. B* **114**, 4271 (2010).
18. A. Banerjee, R. Theron, and R.W.J. Scott: Highly stable noble-metal nanoparticles in tetraalkylphosphonium ionic liquids for in situ catalysis. *ChemSusChem* **5**, 109 (2012).
19. M.F. Mostafa, A.S. Atallah, and M. Elessawi: Preparation and characterization of a new series of perovskite-like structures showing evidence of structural transitions: (methyltriphenylphosphonium)2BX_4, B = Mn, Co, Cu, and Hg, and X = Cl/I. *Phase Transit.* **64**, 215 (1998).
20. M.F. Mostafa and A.S. Atallah: Permittivity and ac conductivity study of the layered perovskite $[(CH_3)\ (C_6H_5)_3P]_2MnCl_4$ showing evidence of phase transition. *Phys. Lett. A* **264**, 242 (1999).
21. M. Schluter, M.L. Cohen, S.E. Kohn, and C.Y. Fong: Electronic structure of BiI_3. *Phys. Status Solidi B* **78**, 737 (1976).
22. J. Coates: Interpretation of infrared spectra, a practical approach. *Encycl. Anal. Chem.* **12**, 10815 (2000).
23. Infrared: Interpretation. https://chem.libretexts.org/Core/Physical_and_Theoretical_Chemistry/Spectroscopy/Vibrational_Spectroscopy/Infrared_Spectroscopy/Infrared%3A_Interpretation.
24. D.A. Skoog, F. James Holler, and T. A. Nieman: *Principios de análisis instrumental*, 5ta Edición (McGraw Hill, Madrid, 2001), p. 409.
25. W. Clegg, R.J. Errington, G.A. Fisher, M.E. Green, D.C.R. Hockless, and N. C. Norman: A phosphine complex of bismuth(III): X-ray crystal structure of $[PMe_3H]$ $[Bi_2Br_7(PMe_3)_2]$. *Chem. Ber.* **124**, 2457 (1991).
26. A. Altomare, C. Cuocci, C. Giacovazzo, A. Moliterni, R. Rizzi, N. Corriero, and A. Falcicchio: EXPO2013: a kit of tools for phasing crystal structures from powder data. *J. Appl. Crystallogr.* **46**, 1231 (2013).
27. D. Winn and M.F. Doherty: Modeling crystal shapes of organic materials grown from solution. *AIChE J.* **46**, 1348 (2000).

https://doi.org/10.1557/mrc.2018.86 Published online by Cambridge University Press